SUPPLEMENTARY ONLINE MATERIALS

Methods 51GGC and 36GGC. Samples were taken for elemental and isotopic analyses at 2 (51GGC) and 4 (36GGC) cm intervals giving a time resolution of 200 to 300 years in each core. Forty *Globigerinoides ruber* shells were collected from the 212 to 250 μm size fraction for elemental measurement. Samples for Mg/Ca were cleaned using the full trace-metal protocol (oxidizing and reducing steps) (Boyle and Keigwin, 1985/6), and elemental ratios measured by ICP-MS (Rosenthal et al., 1999). Mg/Ca was converted to calcification temperature (CT) using a species-specific (*G. ruber*) core top calibration for the Atlantic basin (Dekens et al., 2002):

$$\text{Mg/Ca (mmol/mol)} = 0.38 * \exp(0.09 * CT) \qquad \text{(Eqn.1)}.$$

Due to the shallow depth of the core sites, dissolution likely had no affect on test Mg/Ca (Dekens et al., 2002). Because *G. ruber* lives and calcifies in the surface mixed layer, we consider the *G. ruber* CT a close approximation of sea surface temperature (SST) (Dekens et al., 2002). For 36GGC, seven *G. ruber* shells were selected from 212 to 250 μm size fraction for isotopic analysis. $\delta^{18}O_{calcite}$ was measured on a Finnigan MAT 253 isotope ratio mass spectrometer coupled to a Kiel III carbonate device (Ostermann and Curry, 2000; Lund et al., 2006). Methods for stable isotopic analyses on *G. ruber* from 51GGC are described in Keigwin and Schlegel (2002) and Keigwin (2004). We corrected $\delta^{18}O_{calcite}$ for temperature dependence and removed the effect of continental ice volume on seawater $\delta^{18}O$ (Clark and Mix, 2002) to calculate the sea surface salinity (SSS) dependent $\delta^{18}O_{seawater}$ ($\delta^{18}O_{sw}$). Age models were derived from 13 planktonic radiocarbon dates for 51GGC (Keigwin, 2004) and 14 planktonic and 1 benthic radiocarbon dates for 36GGC (Came et al., 2003). Ages were reservoir corrected, using

1

an additional ΔR of 160 years for 36GGC (CALIB 5.0.2 database), and calibrated with CALIB 5.0.2 with the midpoint chosen for age model construction (Table S1).

Methods GGC5. We sampled GGC5 at ~5 cm intervals and thirty *Globorotalia inflata* shells were collected from the 300 to 355 μm size fraction for elemental measurement. We used *G. inflata* rather than *G. ruber* at GGC5 because of the core depth. *G. inflata* is a larger, more robust foraminifera than *G. ruber* and thus less susceptible to dissolution. Samples for Mg/Ca were cleaned using full trace-metal protocol (Boyle and Keigwin, 1985/6), and elemental ratios measured by ICP-MS (Rosenthal et al., 1999). $\delta^{18}O_{calcite}$ was measured on single *G. inflata* shells using a partially automated VG 903 stable isotope mass spectrometer (McManus et al., 2004). At Bermuda Rise, *G. inlfata* shows little seasonal variability in CT based on multiple trap measurements of $\delta^{18}O_{calcite}$ and its depth habitat is at the thermocline (Anand et al., 2003). Because of the greater depth habitat than *G. ruber*, *G. inflata* could migrate through the water column with temperature change (Anand et al., 2003). Migration would only reduce the CT changes and thus $\delta^{18}O_{sw}$ changes recorded by *G. inflata*; thus our calculations should be seen as minimum values, with the possibility of greater decreases in temperature and increases in $\delta^{18}O_{sw}$ of the water mass. We note that the agreement, but constant offset between $\delta^{18}O_{calcite}$ of *G. inflata* and *G. ruber* at Bermuda Rise (Boyle and Keigwin, 1987; McManus et al., 2004) indicates that *G. inflata* has likely remained in the thermocline through the last deglaciation, without migrating in the water column, thus recording the CT and $\delta^{18}O_{sw}$ of the thermocline.

We corrected $\delta^{18}O_{calcite}$ for temperature dependence from the Mg/Ca CT (see below for Mg/Ca-CT calibration) and removed the effect of continental ice volume on seawater $\delta^{18}O$ (Clark and Mix, 2002) to calculate the SSS dependent $\delta^{18}O_{sw}$. Our age model for GGC5 comes from McManus et al. (2004) who used 13 planktonic reservoir corrected and calibrated radiocarbon dates to establish the core chronology (Table S1).

Because of the water depth of the GGC5 core site (4.55 km), which is actually bathed in deeper Antarctic bottom water from 5.0 km (McCave et al., 1982; Curry and Oppo, 2005), dissolution may affect the Mg/Ca ratio in foraminifera tests, skewing CT estimates toward colder temperatures (Dekens et al., 2002; Benway et al., 2003). To estimate the effects of dissolution as a function of depth, we measured *G. inflata* Mg/Ca in 9 central to western subtropical and northwestern North Atlantic core tops from water depths between 564 m and 4550 m, and also a Bermuda Rise trap sample from 500 to 1500 m water depth (see Table S2 and Fig. S3). We then compared CT calculated from two different calibrations (Elderfield and Ganssen, 2000; Anand et al., 2003) to the predicted CT for *G. inflata* depth and seasonal habitat (Deuser, 1987; Levitus and Boyer, 1994; Hillbrecht, 1996; Elderfield and Ganssen, 2000; Anand et al., 2003). However, neither of these calibrations nor the CT determined from $\delta^{18}O_{calcite}$ produced a GGC5 core top CT in agreement with modern thermocline temperature of the core site. Thus, we devised a new Mg/Ca-CT calibration following Anand et al. (2003) and Dekens et al. (2002):

$$Mg/Ca \ (mmol/mol) = 0.299*exp[0.09*(CT-0.61*D)] \qquad (Eqn. \ 2),$$

where D is the core water depth in km (5 km in the case of GGC5). This is the *G. inflata* Mg/Ca-CT equation derived using sediment trap data from Bermuda (Anand et al., 2003)

with the additional factor -0.61*D added from Dekens et al. (2002) to account for dissolution effects. The species dependence of this equation is in the pre-exponent factor, 0.299, whereas the factor within the exponent parentheses is general to planktonic foraminifera (Dekens et al., 2002; Anand et al., 2003). We test for the effects of dissolution on a sample prior to the use of (Eqn. 2) by comparing the average *G. inflata* test weight of a sample with that of the modern average *G. inflata* sediment trap test weight (see below).

Based on the CT calculated from a north-south North Atlantic transect of *G. inflata* $\delta^{18}O_{calcite}$ (Elderfield and Ganssen, 2000), we infer that *G. inflata* inhabits the upper ~100 m during the spring-summer in the northwestern North Atlantic and the thermocline (~400 m) in the subtropical North Atlantic (Anand et al., 2003). Results from our core top survey suggest that *G. inflata* CT is better estimated by the Elderfield and Ganssen (2000) Mg/Ca-CT equation than by the Anand et al. (2003) Mg/Ca-CT equation, with the exception being the Bermuda Rise core top (GGC5) and sediment trap samples (Fig. S3 & Table S2). To the west and northwest of Bermuda, the Anand et al. equation consistently over predicts CT, whereas the Elderfield and Ganssen equation is within the calibration error and seasonal variability of the CT. We did not find a relationship between Mg/Ca and water depth down to 3890 m, nor is there a relationship between *G. inflata* weight and Mg/Ca (Table S2). At 4550 m water depth of our Bermuda Rise site, however, we do detect the effects of dissolution on Mg/Ca, despite *G. inflata* tests in the Bermuda Rise core top having the greatest average test weight of any of the core top samples (Table S2).

At Bermuda Rise, where *G. inflata* inhabits the thermocline with essentially no seasonal variability, the Elderfield and Ganssen (2000) equation underestimates the CT of the trap *G. inflata* by ~5.7 °C, whereas the Anand et al. (2003) equation overestimates trap *G. inflata* CT by ~1.1 °C (Fig. S3). Given that the Anand et al. equation was developed from Bermuda Rise sediment trap samples (Deuser, 1987), this better agreement is expected. However, both equations underestimate the GGC5 core top CT by ~11 °C (Elderfield and Ganssen, 2000) and ~4.8 °C (Anand et al., 2003), reflecting the effect of dissolution on test Mg/Ca. Using the new equation proposed here that accounts for greater dissolution with greater core water depth, the core top Mg/Ca CT estimate improves to ~15.8 °C, closer to the modern thermocline temperature of 17.5 °C. However, due to lower sedimentation rates during the Holocene relative the last deglaciation at Bermuda Rise, our core top age may not be modern as assumed in the age model construction (McManus et al., 2004). Thus we estimated the CT for core top *G. inflata* of ~16.6 °C (Fig. S3) using the *G. inflata* $\delta^{18}O_{calcite}$, an assumed salinity of 36.45 practical salinity units and the modern salinity-$\delta^{18}O_{sw}$ relationship for Bermuda Rise (Anand et al., 2003; LeGrande and Schmidt, 2006). This CT of ~16.6 °C is within the Mg/Ca-CT calibration error of ± 1.6 °C (see below). In addition, our predicted $\delta^{18}O_{sw}$ for the core top from the Mg/Ca CT and *G. inflata* $\delta^{18}O_{calcite}$ is ~1.07 per mil in excellent agreement with the modern $\delta^{18}O_{sw}$ for Bermuda Rise of ~1.11 per mil (LeGrande and Schmidt, 2006).

We note that this is a constant correction for dissolution, which may have varied in the past. However, given that the current core site is already bathed in Antarctic bottom water, any reduction in Atlantic meridional overturning circulation (AMOC)

strength would not change the water mass directly overlying the core site as much as it would if the core were shallower (Curry and Oppo, 2005). Thus past reductions in AMOC likely have not imprinted themselves significantly on the dissolution history at GGC5. During the early Holocene, better preservation of carbonate in the ocean due to the out-gassing of carbon dioxide (i.e. Berger, 1977) allowed for little to no dissolution of *G. inflata* tests at Bermuda Rise, evident in a peak in *G. inflata* test weight (Fig. S4). Thus we use average *G. inflata* test weight in GGC5 to detect if dissolution occurred. If the sample has an average *G. inflata* test weight less than the modern sediment trap weight suggesting dissolution, we use (Eqn. 2) to calculate CT. If the sample has an average *G. inflata* test weight greater than the modern sediment trap weight suggesting no dissolution, we use the Anand et al. (2003) *G. inflata* equation to calculate CT:

$$\text{Mg/Ca (mmol/mol)} = 0.299*\exp(0.09*CT) \qquad \text{(Eqn. 3)}.$$

Indeed, during the early Holocene when *G. inflata* test weights were greater than modern trap test weights (Fig. S4), the Anand et al. (2003) equation calculates CT of ~18.5 ºC in excellent agreement with the CT calculated from $\delta^{18}O_{calcite}$ of ~18.7 ºC (Fig. S4). We note that the use of these two equations to calculate CT does not affect our deglacial record and inferences there from, because all deglacial *G. inflata* test weights are less than the modern core top weight and thus we use a consistent Mg/Ca-CT equation.

Error Analysis. Duplicate *G. ruber* and *G. inflata* Mg/Ca measurements suggest a Mg/Ca CT analytical precision of ± 0.12 mmol/mol (± 0.4 ºC). The standard error of the calibration for *G. ruber* is larger (± 1.2 ºC) (Dekens et al., 2002) but this only affects the absolute temperature, not the estimated change in CT. While we do not have a precisely

determined standard error for the *G. inflata* Mg/Ca-CT calibration used here, we suggest a conservative estimate of ± 1.2 ºC (i.e. Dekens et al., 2002; Anand et al., 2003). Thus final CT values have an absolute error of ± 1.6 ºC including the measurement precision and calibration error. $\delta^{18}O_{calcite}$ has a long-term reproducibility of ± 0.08 per mil (McManus et al., 2004; Lund et al., 2006). We use Monte Carlo methods assuming a normal distribution in the analytical precision of Mg/Ca, $\delta^{18}O_{calcite}$ and Mg/Ca-CT calibration to determine the $\delta^{18}O_{sw}$ precision of ± 0.26 per mil for absolute $\delta^{18}O_{sw}$. For comparisons between samples from the same core (e.g. not including the calibration uncertainty), $\delta^{18}O_{sw}$ precisions is ± 0.12 per mil. We do not consider the effect of salinity on foraminifera Mg/Ca, where increased salinity increases the Mg/Ca ratio in the test. However, this effect is relatively small (~4 %) when compared to the influence of temperature on test Mg/Ca (Lea et al., 1999).

Resolution of the records. GGC5 has a relatively constant sample resolution through the last deglaciation with two exceptions (Fig. S1a, b & c). First, the core only extends to ~20 k.y. B.P., near the end of the Last Glacial Maximum (Clark and Mix, 2002). Second, the latter part of the Younger Dryas cold period 12-11.5 k.y. B.P. is less well resolved with only 3 samples. The only interval in 51GGC with lower sample resolution is from 21-17 k.y. B.P. due to the low sedimentation rates at the core site (Fig. S1d, e & f), with 5 samples in this 4 k.y. period. The sample resolution of 36GGC is relatively constant through out the last deglaciation, with only slightly lower resolution from ~13-11 k.y. B.P. (Fig. S1g, h & i).

Influence of CT versus $\delta^{18}O_{calcite}$ on $\delta^{18}O_{sw}$ records. The $\delta^{18}O_{sw}$ records generally mimic the $\delta^{18}O_{calcite}$ records, especially in the case of GGC5 and 51GGC (Fig. S1). In GGC5, $\delta^{18}O_{calcite}$ and $\delta^{18}O_{sw}$ are similar, though coincident CT cooling with increases in $\delta^{18}O_{calcite}$ reduces the magnitude of $\delta^{18}O_{sw}$ increases centered at ~17, 15 and 13 k.y. B.P. (Fig. S1a, b & c). In contrast, CT warming in 51GGC from ~20 to 15 k.y. B.P. increases the concurrent $\delta^{18}O_{sw}$ increase (Fig. S1d, e & f). Similarly, CT cooling from ~15 to 13 k.y. B.P. amplifies the contemporaneous $\delta^{18}O_{sw}$ decrease. For 36GGC, CT warming from ~15 to 13 k.y. B.P. augments the decrease in $\delta^{18}O_{sw}$ (Fig. S1g, h & i).

Core Top Records. Our late-Holocene CT estimates are 26 ± 1.6 °C for 51GGC, 22 ± 1.6 °C for 36GGC, and 15.8± 1.6 °C for GGC5. The 51GGC CT is in agreement with the modern average summer SST of 27 °C. The 36GGC estimate is cooler than the average austral summer SST of 24 °C. However, the core top age is 1,114 ± 64 cal yrs BP (Came et al., 2003) indicating that the CT is from an earlier cooler period of earth history. GGC5 is within error of the modern thermocline temperature of 17.5 °C, and closer to the $\delta^{18}O_{calcite}$ estimated CT of ~16.6 °C (Fig. S3). Late Holocene values for $\delta^{18}O_{sw}$ of ~1.07 per mil (GGC5), ~0.4 per mil (51GGC) and ~0.6 per mil (36GGC) are in agreement with modern surface $\delta^{18}O_{sw}$ of these regions (LeGrande and Schmidt, 2006).

References

Anand, P., Elderfield, H., and Conte, M.H., 2003, Calibration of Mg/Ca thermometry in planktonic foraminifera from a sediment trap time series: Paleoceanography, v. 18, doi: 10.1029/2002PA000846.

Benway, H.M., Haley, B.A., Klinkhammer, G.P., and Mix, A.C., 2003, Adaptation of a flow-through leaching procedure for Mg/Ca paleothermometry: Geochemistry, Geophysics, Geosystems, v. 4, doi: 10.1029/2002GC000312.

Berger, W.H., 1977, Deep-sea carbonate and the deglaciation preservation spike in pteropods and foraminifera: Nature, v. 269, p. 301-304.

Boyle, E.A., and Keigwin, L.D., 1985/6, Comparison of Atlantic and Pacific paleochemical records for the last 215,000 years: changes in deep ocean circulation and chemical inventories: Earth and Planetary Science Letters, v. 76, p. 135-150.

Boyle, E.A., and Keigwin, L.D., 1987, North Atlantic thermohaline circulation during the past 20,000 years linked to high-latitude surface temperature: Nature, v. 330, p. 35-40.

Came, R.E., Oppo, D.W., and Curry, W.B., 2003, Atlantic Ocean circulation during the Younger Dryas: Insights from a new Cd/Ca record from the western subtropical South Atlantic: Paleoceanography, v. 18, doi: 10.1029/2003PA000888.

Clark, P.U., and Mix, A.C., 2002, Ice sheets and sea level of the Last Glacial Maximum: Quaternary Science Reviews, v. 21, p. 1-7.

Curry, W.B., and Oppo, D.W., 2005, Glacial water mass geometry and the distribution of d13C and ZCO2 in the western Atlantic Ocean: Paleoceanography, v. 20, doi: 10.1029/2004PA001021.

Dekens, P.S., Lea, D.W., Pak, D.K., and Spero, H.J., 2002, Core top calibration of Mg/Ca in tropical foraminifera: Refining paleotemperature estimation: Geochemistry, Geophysics, Geosystems, v. 3, doi: 10.1029/2001GC000200.

Deuser, W.G., 1987, Seasonal variations in isotopic composition and deep-water fluxes of the tests of perennially abundant planktonic foraminifera of the Sargasso Sea: Results from sediment trap collections and their paleoceanographic significance: Journal of Foraminiferal Research, v. 17, p. 268-293.

Elderfield, H., and Ganssen, G., 2000, Past temperature and $\delta^{18}O$ of surface ocean waters inferred from foraminiferal Mg/Ca ratios: Nature, v. 405, p. 442-445.

Hillbrecht, H., 1996, Extant planktic foraminifera and the physical environment in the Atlantic and Indian Oceans: Mitteilungen aus dem Geologischen Institut der Eidgen, Technischen Hochschule und der Universität Zürich, Neue Folge. No. 300, 93 pp.

Keigwin, L.D., 2004, Radiocarbon and stable isotope constraints on Last Glacial Maximum and Younger Dryas ventilation in the western North Atlantic: Paleoceanography, v. 19, doi: 10.1029/2004PA001029.

Keigwin, L.D., and Schlegel, M.A., 2002, Ocean ventilation and sedimentation since the glacial maximum at 3 km in the western North Atlantic: Geochemistry, Geophysics, Geosystems, v. 3, doi: 10.1029/2001GC000283.

Lea, D.W., Mashiotta, T.A., and Spero, H.J., 1999, Controls on magnesium and strontium uptake in planktonic foraminifera determined by live culturing: Geochimica et Cosmochimica Acta, v. 63, p. 2369-2379.

LeGrande, A.N., and Schmidt, G.A., 2006, Global gridded data set of the oxygen isotopic composition in seawater: Geophysical Research Letters, v. 33, doi: 10.1029/2006GL026011.

Levitus, S., and Boyer, T., 1994, World Ocean Atlas 1994 Volume 4: Temperature: NOAA Atlas NESDIS 4, U.S. Department of Commerce, Washington, D.C.

Lund, D.C., Lynch-Stieglitz, J., and Curry, W.B., 2006, Gulf Stream density structure and transport during the past millennium: Nature, v. 444, p. 601-604.

McCave, I.N., Hollister, C.D., Laines, E.P., Lonsdale, P.F., and Richardson, M.J., 1982, Erosion and deposition on the eastern margin of the Bermuda Rise in the late Quaternary: Deep Sea Research, v. 29, p. 535-561.

McManus, J.F., Francois, R., Gherardi, J.-M., Keigwin, L.D., and Brown-Ledger, S., 2004, Collapse and rapid resumption of Atlantic meridional circulation linked to deglacial climate changes: Nature, v. 428, p. 834-837.

Ostermann, D.R., and Curry, W.B., 2000, Calibration of stable isotopic data: An enriched $\delta^{18}O$ standard used for source gas mixing detection and correction: Paleoceanography, v. 15, p. 353-360.

Rosenthal, Y., Field, P., and Sherrell, R., 1999, Precise determination of element/Calcium ratios in calcareous samples using Sector Field Inductively Coupled Plasma Mass Spectrometry: Analytical Chemistry, v. 71, p. 3248-3253.

Core	Depth (cm)	^{14}C age	± Error	Calibrated age	± 2 σ
GGC5	65	5420	60	6240	70
GGC5	97	9650	40	11130	70
GGC5	112	10450	55	12390	260
GGC5	127	11900	50	13770	120
GGC5	137	12250	50	14130	180
GGC5	137	12300	50	14290	280
GGC5	161	12400	50	14460	330
GGC5	207	13900	150	16560	500
GGC5	221	14350	65	17150	440
GGC5	257	14800	80	18070	440
GGC5	261	15100	70	18540	140
GGC5	400	16450	80	19640	180
GGC5	407	16800	90	20000	200
51GGC	210	6910	55	7760	100
51GGC	280	9700	55	11150	80
51GGC	290	9800	55	11220	100
51GGC	300	10300	60	12170	220
51GGC	310	10950	65	12930	100
51GGC	320	11550	60	13410	150
51GGC	330	11850	100	13680	240
51GGC	350	12750	85	15040	330
51GGC	360	13900	85	16560	410
51GGC	370	14350	80	17170	470
51GGC	380	17700	110	20910	390
51GGC	400	19800	130	23710	440
51GGC	410	23200	190	25120	500
36GGC	1	1180	30	1110	60
36GGC	16	2610	60	2770	90
36GGC	28	3890	40	4320	100
36GGC	40	5440	35	6240	50
36GGC	56	7950	50	8820	180
36GGC	60	8890	50	10040	150
36GGC	68	10040	45	11540	220
36GGC	80	10840	50	12850	50
36GGC	88	11640	50	13500	150
36GGC	92	11890	60	13760	150
36GGC	104	12990	60	15370	310
36GGC	112	13090	60	15500	330
36GGC	141	14290	120	17160	600
36GGC	148	15490	65	18800	120
36GGC	200	18740	95	22300	180

Table S1. Radiocarbon dates (reservoir corrected using CALIB 5.0.2 database) used in age model reconstruction, calibrated with CALIB 5.0.2.

Core Top & Trap	Depth (m)	Lat. N	Lon. W	Shell wt (μg)	Mg/Ca (mmol/mol)	CT Anand	CT E&G	T 400m	T 100m	T 50m	T 0m
Bermuda Trap	500-1500	32.09	64.26	28	1.59	18.6	11.8	17.5	19-21	21-25	21-27
GGC5	4550	33.70	57.58	27	0.94	12.7	6.5	17.5	19-21	21-25	21-27
51GGC	1790	32.78	76.28	23	1.99	21.1	14.0	15	21-22	21-25	21-28
4PC	1629	42.70	61.65	24	1.45	17.5	10.8	7	9-11	7-13	7-19
MC13A	3440	43.07	55.83	26	1.42	17.3	10.6	6.5	7-8	5-11	5-19
PC7	920	43.35	60.22	21	1.09	14.4	8.0	6	7-8	5-10	4-18
PC7	920	43.35	60.22	23	1.10	14.5	8.1	6	7-8	5-10	4-18
MC25B	3890	43.48	54.87	23	1.28	16.2	9.6	6.5	7-8	5-10	5-18
119PC	2080	43.75	58.29	21	1.26	16.0	9.4	6	7-8	6-11	5-19
5R	900	44.42	53.67	27	1.15	15.0	8.6	4.5	3-4	2-6	2-17
10PC	564	44.84	55.98	19	0.90	12.3	6.1	5	4-5	3-7	2-17

Table S2. Table of core top and Bermuda sediment trap Mg/Ca values for *G. inflata*. Core depth, location, average *G. inflata* weight, measured Mg/Ca, calculated calcification temperature (CT) using Anand et al. (2003) (Anand) and Elderfield and Ganssen (2000) (E&G), and seasonal temperature range at core sites from 400 (400 m has no seasonal variability), 100, 50 and 0 m water depths (Levitus and Boyer, 1994). Core tops are as follows: GGC5 = OCE326-GGC5, 51GGC = KNR140-51GGC, 4PC = DW83-012-4PC, MC13A = OCE326-MC13A, PC7 = HUD87-003-PC7, MC25B = OCE326-MC25B, 119PC = HUD75-009-119PC, 5R = HUD86-013-5R, 10PC = DW84-003-10PC.

13

Age (k.y. B.P.)	Mg/Ca (mmol/mol)	CT	$\delta^{18}O_{calcite}$	$\delta^{18}O_{sw}$
0.37			-1.62	
0.74			-1.70	
1.11			-1.82	
1.48			-1.85	
1.85			-1.76	
2.22			-1.69	
2.59			-1.59	
2.96			-1.63	
3.33			-1.55	
3.70			-1.55	
4.06			-1.45	
4.43			-1.54	
4.80			-1.51	
5.17			-1.50	
5.54			-1.48	
5.91			-1.59	
6.28			-1.56	
6.65			-1.59	
7.02			-1.62	
7.39			-1.85	
7.76	4.46	27.38	-1.64	0.71
8.24	4.96	28.54	-1.45	1.37
8.73	4.56	27.62	-1.34	0.89
9.21	4.24	26.79	-1.42	0.79
9.70	4.75	28.06	-1.30	0.89
10.18	4.56	27.60	-1.33	1.11
10.67	4.16	26.60	-1.26	0.54
11.15	4.06	26.32	-1.33	0.62
11.16	4.16	26.59	-1.28	0.63
11.19	3.90	25.88	-1.16	0.51
11.21	3.79	25.55	-1.10	0.81
11.22	4.21	26.73	-1.11	0.86
11.60	3.96	26.04	-1.22	0.51
11.98	3.82	25.63	-1.11	0.45
12.17	3.75	25.45	-0.92	0.90
12.32	4.60	27.71	-0.70	1.39
12.62	3.74	25.42	-0.60	1.02
12.93	3.79	25.54	-0.46	1.14
13.03	3.40	24.33	-0.31	1.08
13.22	4.20	26.70	-0.24	1.73
13.41	4.04	26.27	-0.33	1.45
13.52	3.34	24.15	-0.57	0.72
13.63	3.42	24.43	-0.57	0.48
13.68	3.96	26.04	-0.55	1.35
13.82	3.68	25.22	-0.41	0.97
14.09	3.54	24.78	-0.47	0.89
14.36	4.19	26.67	-0.36	1.18
14.50	3.70	25.29	-0.30	1.20
14.63	3.63	25.09	-0.40	1.09

14.90	3.46	24.55	-0.67	0.40
15.04	4.54	27.55	-0.61	0.83
15.34	4.91	28.42	-0.32	1.92
15.95			-0.13	
16.56	4.47	27.39	-0.13	1.28
16.81	4.29	26.94	-0.26	1.56
17.05	3.54	24.78	-0.07	0.83
17.17	4.73	28.02	-0.06	1.95
17.92	3.99	26.13	-0.03	1.37
19.42	4.28	26.92	-0.11	1.14
20.91	4.13	26.95	0.32	1.77
22.31	3.61	25.02	0.25	1.18
23.71	3.66	25.17	0.25	1.39
25.12	3.84	25.69	0.57	1.72

Table S3. 51GGC Mg/Ca, calcification temperature (CT), $\delta^{18}O_{calcite}$ and $\delta^{18}O_{sw}$ data on age model scale.

Age (k.y. B.P.)	Mg/Ca (mmol/mol)	CT	$\delta^{18}O_{calcite}$	$\delta^{18}O_{sw}$
1.11			-1.08	
1.44			-0.91	
1.88			-0.87	
2.32			-0.94	
2.77			-1.01	
3.28			-0.68	
3.80			-0.81	
4.32			-0.61	
4.96			-0.72	
5.60			-0.84	
6.24			-0.93	
6.89			-0.61	
7.53			-0.66	
8.17			-0.48	
8.82			-0.64	
9.72	3.65	25.15	-0.23	1.55
10.63	3.64	25.11	-0.16	1.50
11.54	3.78	25.52	-0.17	1.52
11.98	3.76	25.46	-0.33	1.33
12.41	3.83	25.66	-0.24	1.44
12.85	3.69	25.24	-0.25	1.31
13.17	3.71	25.33	0.32	1.90
13.50	3.79	25.54	0.18	1.70
13.76	3.54	24.81	0.17	1.52
14.30	3.25	23.85	0.20	1.29
14.83	3.35	24.17	0.20	1.32
15.37	3.01	22.99	0.38	1.23
15.43	3.11	23.37	0.34	1.27
15.50	3.17	23.56	0.38	1.34
15.73	3.43	24.45	0.68	1.81
15.97	3.38	24.30	0.25	1.59
16.21	3.21	23.70	0.03	1.65
16.45	3.41	24.39	0.48	1.78
16.68	3.53	24.76	0.74	2.13
16.92	3.05	23.12	0.75	1.55
17.16	3.06	23.17	0.79	1.59
17.98	3.91	25.89	0.83	2.15
18.80	3.44	24.48	0.29	1.29
19.07	3.23	23.77	0.40	1.18
19.34	3.16	23.55	0.53	1.19
19.61	3.38	24.28	0.66	1.49
19.88	3.51	24.70	0.49	1.42
20.15	3.11	23.34	0.54	1.21
20.41	2.92	22.67	0.39	0.93
20.68	3.66	25.17	0.28	1.35

20.95	3.36	24.23	0.47	1.35
21.49	3.17	23.58	0.46	1.18
22.03	3.10	23.33	0.67	1.33
22.30	3.13	23.43	0.39	1.07
22.84	3.10	23.34	0.72	1.38

Table S4. 36GGC Mg/Ca, calcification temperature (CT), $\delta^{18}O_{calcite}$ and $\delta^{18}O_{sw}$ data on age model scale.

Age (k.y. B.P.)	Mg/Ca (mmol/mol)	CT	$\delta^{18}O_{calcite}$	$\delta^{18}O_{sw}$
0.57	0.94	15.75	0.88	0.99
2.10	1.07	17.26	0.74	1.16
4.01	1.00	16.49	0.61	0.86
6.11	0.96	15.99	0.90	1.03
7.33	1.05	16.95	0.69	0.95
8.08	1.21	18.54	0.58	1.13
8.83	1.20	18.48	0.36	0.85
9.58	1.58	18.51	0.38	0.80
10.33	1.39	17.05	0.40	0.41
11.05	1.50	17.96	0.18	0.32
11.54	1.45	17.55	0.37	0.40
12.04	0.82	14.27	0.78	0.11
12.53	0.79	13.78	1.83	1.03
13.02	0.83	14.39	1.78	1.07
13.52	0.92	15.56	1.22	0.71
13.99	1.01	16.53	0.66	0.30
14.25	0.84	14.58	1.13	0.31
14.51	0.85	14.69	1.34	0.50
14.76	0.61	10.98	2.17	0.55
15.04	0.62	11.20	1.98	0.39
15.23	0.75	13.28	2.03	0.86
15.51	0.82	14.22	2.01	1.03
15.79	0.92	15.56	1.08	0.36
16.08	0.93	15.64	1.54	0.82
16.17	0.89	15.11	1.55	0.72
16.26	0.80	13.95	1.58	0.50
16.51	0.89	15.23	2.23	1.41
16.75	0.71	12.59	2.64	1.26
17.05	0.77	13.62	2.77	1.59
17.26	0.73	13.01	2.47	1.15
17.52	0.68	12.22	2.85	1.35
17.72	0.82	14.26	3.04	1.95
18.06	0.89	15.19	1.90	1.00
18.24	0.90	15.32	1.68	0.80
18.52	0.90	15.26	1.75	0.86
18.76	0.66	11.78	1.47	-0.17
19.00	1.23	18.74	1.68	1.46
19.25	0.73	12.93	1.68	0.21
19.51	0.87	14.97	2.07	1.00
19.68	0.93	15.64	1.77	0.83
19.79	0.83	14.34	1.81	0.60
19.91	0.84	14.49	1.72	0.53

Table S5. GGC5 Mg/Ca, calcification temperature (CT), $\delta^{18}O_{calcite}$ and $\delta^{18}O_{sw}$ data on age model scale.
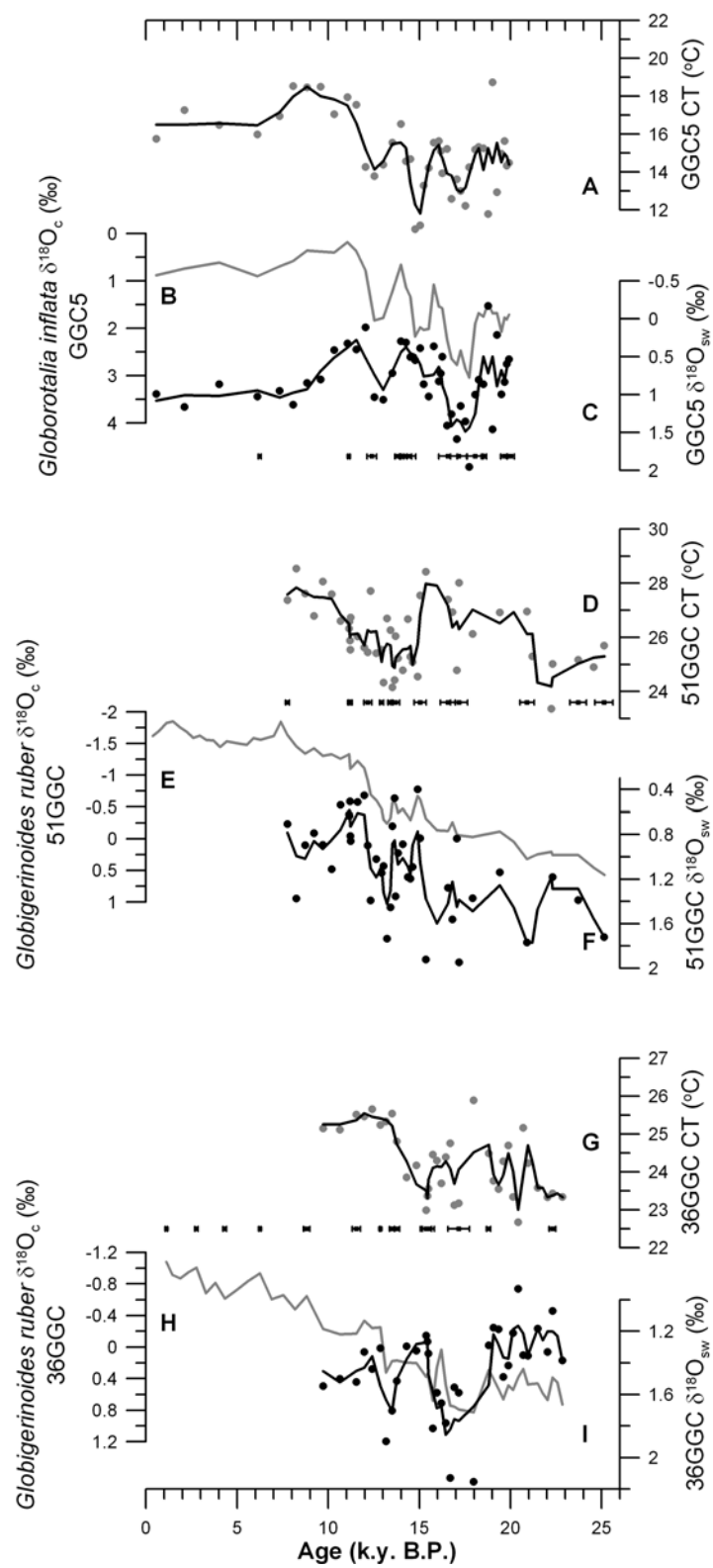
Supplementary Figure S1. Mg/Ca-CT, $\delta^{18}O_{calcite}$ ($\delta^{18}O_c$) and $\delta^{18}O_{seawater}$ ($\delta^{18}O_{sw}$) from GGC5 (**a-c**), 51GGC (**d-f**), and 36GGC (**g-i**). (**a**) GGC5 *G. inflata* CT (gray dots) with 3-point smoothing (black line). (**b**) GGC5 *G. inlfata* $\delta^{18}O_c$ (gray line). (**c**) GGC5 $\delta^{18}O_{sw}$ (black dots) with 3-point smoothing (black line). (**d**) 51GGC *G. ruber* CT (gray dots) with 3-point smoothing (black line). (**e**) 51GGC *G. ruber* $\delta^{18}O_c$ (gray line). (**f**) 51GGC $\delta^{18}O_{sw}$ (black dots) with 3-point smoothing (black line). (**g**) 36GGC *G. ruber* CT (gray dots) with 3-point smoothing (black line). (**h**) 36GGC *G. ruber* $\delta^{18}O_c$ (gray line). (**i**) 36GGC $\delta^{18}O_{sw}$ (black dots) with 3-point smoothing (black line). Black boxes denote radiocarbon age control (Came et al., 2003; Keigwin, 2004; McManus et al., 2004).

Supplementary Figure S2. Change $\delta^{18}O_{precipitation}$ ($\delta^{18}O_{prec}$) in NASA Goddard Institute for Space Studies ModelE-R in response to 0.1 Sverdrup × 100 years freshwater forcing to the North Atlantic with an ~50% reduction in AMOC strength (average of the last 20 years) for the tropical, northern and southern subtropical Atlantic. Note the increase in $\delta^{18}O_{prec}$ in the northern tropics and reduction in the southern tropics related to the southward migration of the intertropical convergence zone (ITCZ). Black line denotes zero change in $\delta^{18}O_{prec}$.
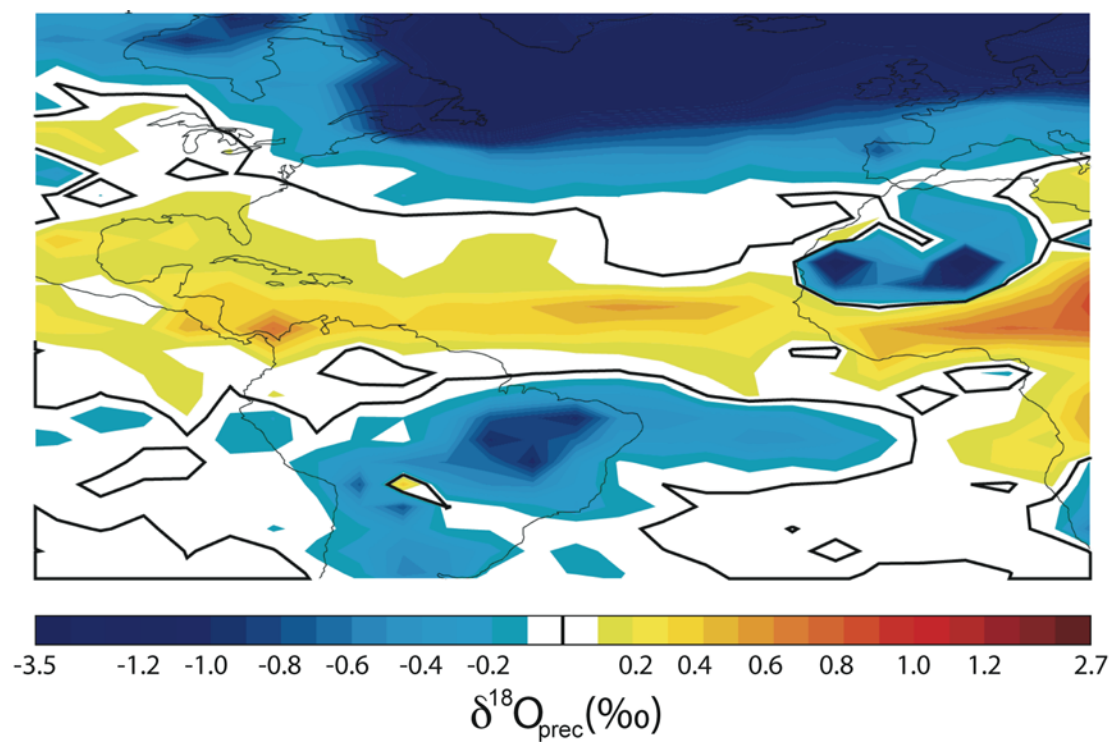
Supplementary Figure S3. North Atlantic *G. inflata* core top Mg/Ca calcification temperature (CT) and seasonal temperature variability for inferred calcification depth (Levitus and Boyer, 1994); 400 m for subtropical sites, 100 to 50 m for northwestern Atlantic sites. Data and full core names are given in Table S1. Mg/Ca CT was calculated using the calibrations of Anand et al. (2003) (gray circles) and Elderfield and Ganssen (2000) (black diamonds). Also shown is the CT calculated from the core top $\delta^{18}O_c$ of *G.*

inflata at GGC5 (black square) versus GGC5 CT from Mg/Ca using the revised *G. inflata* calibration of this study.
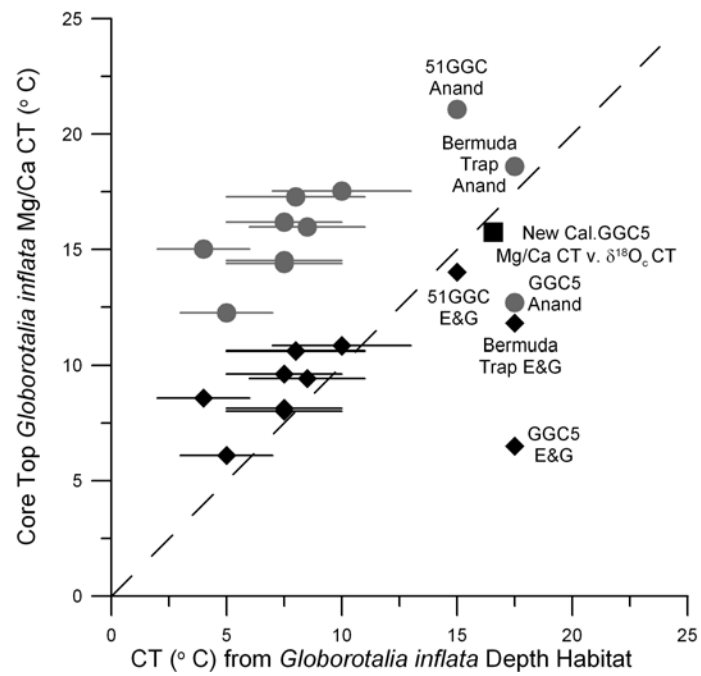
Supplementary Figure S4. (**a**) GGC5 Mg/Ca record (black line with triangle symbols), with gray boxes denoting samples that likely did not experience dissolution (e.g. the Anand et al. (2003) equation was used to calculate CT (**a**). All other samples used (Eqn. 1) to calculate CT. (**b**) $\delta^{18}O_c$ record. (**c**) *G. inflata* test weight. Dashed horizontal gray line denotes cutoff for samples that have experienced dissolution (weights below modern sediment trap weights) and samples that have not experienced dissolution (weights heavier than modern sediment trap weights).
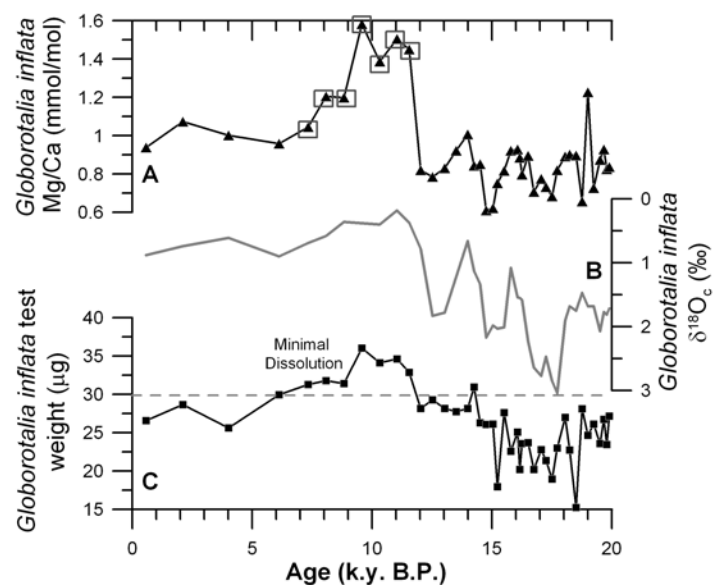
Supplementary Figure S1

Supplementary Figure S2

Supplementary Figure S3

Supplementary Figure S4